Investigating the Unique Properties of Cuphea-Derived Biodiesel Fuel with the Advanced Distillation Curve Method

Tara M. Lovestead, Bret C. Windom, and Thomas J. Bruno*

Thermophysical Properties Division, National Institute of Standards and Technology (NIST), Boulder, Colorado 80305

Currently, there is a desire to extend or enhance petroleum-derived diesel fuel with biodiesel fuel. Biodiesel fuel is a renewable, biomass-derived fluid that is biodegradable and nontoxic and can impart increased lubricity to petroleum-derived diesel fuels. In this paper, we analyze the properties of two biodiesel fuels produced from different feedstocks by use of the advanced distillation curve (ADC) method. The biodiesel fuels include a soybean-derived biodiesel fuel, SME, and a cuphea-derived biodiesel fuel, CME. Specifically, we present the thermodynamically consistent distillation curves and use the composition channel to characterize the curves in terms of composition and available energy content. This work provides a basis of comparison among these fuels in terms of the fundamental thermophysical properties. This comparison will be critical in determining the applicability and suitability of feedstocks designed for the production and manufacturing of biodiesel fuel to enhance or extend current petroleum-derived diesel fuels.

Introduction

Biodiesel Fuel. Current research on alternative fuels, driven by diminishing petroleum reserves, the potential of supply disruptions and price volatility, as well as environmental considerations, has led to the development of alternative liquid fuels produced from renewable feedstocks. An alternative fuel is any fuel that can be made from a material or substance, such as biomass (plant matter, algae, fats, oils, and other lipids), that is a nonfossil and inherently renewable.[1] Several alternative fuels can be used as extenders and/or enhancers for petroleum-derived diesel fuel. Biodiesel fuel is one such alternative that can be derived from a number of feedstocks, including plant and vegetable oils, algae, animal fats, waste oils, etc.[2] Biodiesel fuel is biodegradable and nontoxic and can impart increased lubricity to petroleum-derived diesel fuels.[1] Additional benefits to the use of biodiesel fuel include reduced particulate matter and reduced emissions of toxic compounds.[3] On the other hand, some of the known problems with biodiesel fuel include potential for poor oxidative stability, poor low-temperature operability (higher cloud point), microbial contamination, a possible increase in NO_x emissions for some engines, and limited supply.[2−6]

A number of feedstocks are currently used to produce oils that can be processed into biodiesel fuel. Soybean, palm, rapeseed, sunflower seed, coconut, peanut, and cottonseed oils, along with animal fats and waste oils, have all been proven to be viable feedstock sources.[7,8] Typically, the feedstock that is selected depends upon the crop economics, geography, climate, and crop availability.[1,9] For example, most of the biodiesel fuel produced within the United States is derived from soybean, whereas in countries with tropical climates, biodiesel fuel is derived from palm and coconut oil. To improve and/or expand the production of biodiesel fuel alternative feedstocks, such as algae, jatropha, coffee grounds, tobacco, wild Brazilian mustard seed, coriander seed, field pennycress, cuphea, etc., are being investigated.[2,9−15]

(7) Stroup, R. L. Feedstock considerations for future U.S. producers. *Biodiesel Magazine* **2004**.
(8) Soyatech. 2008 Soya and Oilseed Bluebook, 2007; ISSN , p 346.
(9) Moser, B. R.; Vaughn, S. F. Coriander seed oil methyl esters as biodiesel fuel: Unique fatty acid composition and excellent oxidative stability. *Biomass Bioenergy* **2010**, *34* (4), 550–558.
(10) Jham, G.; Moser, B.; Shah, S.; Holser, R.; Dhingra, O.; Vaughn, S.; Berhow, M.; Winkler-Moser, J.; Isbell, T.; Holloway, R.; Walter, E.; Natalino, R.; Anderson, J.; Stelly, D. Wild Brazilian mustard seed oil methyl esters as biodiesel fuel. *J. Am. Oil Chem. Soc.* **2009**, *86*, 917–926.
(11) Kondamudi, N.; Mohapatra, S. K.; Misra, M. Spent coffee grounds as a versatile source of green energy. *J. Agric. Food Chem.* **2008**, *56* (24), 11757–11760.
(12) Tiwari, A.; Kumar, A.; Raheman, H. Biodiesel production from jatropha oil (*Jatropha curcas*) with high free fatty acids: An optimized process. *Biomass Bioenergy* **2007**, *31*, 569–575.
(13) Usta, N. Use of tobacco seed oil methyl ester in a turbocharged indirect injection diesel engine. *Biomass Bioenergy* **2005**, *28* (1), 77–86.
(14) Johnson, M. B.; Wen, Z. Production of biodiesel fuel from the microalga *Schizochytrium limacinum* by direct transesterification of algal biomass. *Energy Fuels* **2009**, *23* (10), 5179–5183.
(15) Moser, B.; Knothe, G.; Vaughn, S. F.; Isbell, T. A. Production and evaluation of biodiesel from field pennycress (*Thlaspi arvense* L.) oil. *Energy Fuels* **2009**, *23*, 4149–4155.

*To whom correspondence should be addressed. Telephone: 303-497-5158. Fax: 303-497-5044. E-mail: bruno@boulder.nist.gov.

(1) Knothe, G.; Krahl, J.; Van Gerpen, J. *The Biodiesel Handbook*; American Oil Chemists' Society (AOCS) Press: Champaign, IL, 2005.
(2) Knothe, G.; Cermak, S. C.; Evangelista, R. L. Cuphea oil as source of biodiesel with improved fuel properties caused by high content of methyl decanoate. *Energy Fuels* **2009**, *23*, 1743–1747.
(3) Moser, B. R.; Williams, A.; Haas, M. J.; McCormick, R. L. Exhaust emissions and fuel properties of partially hydrogenated soybean oil methyl esters blended with ultra low sulfur diesel fuel. *Fuel Process. Technol.* **2009**, *90* (9), 1122–1128.
(4) McCormick, R. L.; Ratcliff, M.; Moens, L.; Lawrence, R. Several factors affecting the stability of biodiesel in standard accelerated tests. *Fuel Process. Technol.* **2007**, *88* (7), 651–657.
(5) McCormick, R. L. The impact of biodiesel on pollutant emissions and public health. *Inhalation Toxicol.* **2007**, *19* (12), 1033–1039.
(6) Haas, M. J.; Scott, K. M.; Alleman, T. L.; McCormick, R. L. Engine performance of biodiesel fuel prepared from soybean soapstock: A high quality renewable fuel produced from a waste feedstock. *Energy Fuels* **2001**, *15* (5), 1207–1212.

Table 1. Property Information for the FAME Compounds Discussed Herein[a]

FAME	CAS number	RMM	BP (°C)	MP (°C)
methyl caprylate, C8:0	111-11-5	158.24	192.95 (0.35)[83]	−37.43 (0.26)
methyl caprate, C10:0	110-42-9	186.29	224.1 (1.0)[83]	−13.48 (0.52)
methyl laurate, C12:0	111-82-0	214.34	266.9 (13.3)[81]	4.3 (0.54)
methyl myristate, C14:0	124-10-7	242.4	323.1 (2.0)[84]	18.00 (0.42)
methyl palmitate, C16:0	112-39-0	270.45	331.9 (3.3)[85]	28.48 (0.44)
methyl stearate, C18:0	112-61-8	298.5	360.9 (18.0)[85]	37.66 (0.25)
methyl oleate, C18:1 $\Delta 9c$	112-62-9	296.49	343.9 (34.4)[81]	−20.21 (0.51)
methyl vaccenate, C18:1 $\Delta 11c$	1937-63-9	296.49	not available	−24.29 (0.72)
methyl linoleate, C18:2 $\Delta 9c$, $\Delta 12c$	112-63-0	294.47	346.0 (10.4)[86]	−43.09 (0.71)
methyl linolenate, C18:3 $\Delta 9c$, $\Delta 12c$, $\Delta 15c$	301-00-8	292.46	347.0 (10.4)[86]	−57.0 (0.57)[87]

[a] Additional notation is included to indicate the position and orientation of the double bond(s), where $\Delta 9c$ is a double bond at the 9th carbon in the cis configuration. Unless otherwise marked, the melting points (MP) were determined experimentally by Knothe and Dunn by differential scanning calorimetry.[19] BP is the normal boiling point (BP). In some cases, the references are as given in the NIST Chemistry WebBook.[82] RMM is the relative molecular mass of the compound. The uncertainties are provided in parentheses.

The properties of the biodiesel fuel, including cold flow properties, oxidative stability, and energy content, are dependent upon the feedstock used.[9,16] For example, biodiesel fuel made from soybean oil has a lower cloud point temperature (~1 °C) compared to that of palm oil (~17 °C).[17,18] Furthermore, coconut oil has a lower cloud point temperature (~ −5 °C) compared to those of both soybean and palm oils. The different properties exhibited by biodiesel fuels made from different feedstocks are primarily due to the fatty acids that make up the feedstock oil. The fatty acid profile (the chain-length distribution and the degree of unsaturation) determines the fatty acid methyl ester (FAME) profile of the resulting biodiesel fuel and, thus, its properties. To illustrate this concept, we can discuss three common feedstocks for biodiesel fuel production: soybean, palm, and coconut oils. Biodiesel fuels made from coconut oil are composed of primarily medium-size FAMEs, ~50% C12:0 and 15% C14:0, where 12 and 14 are the number of carbons in the fatty acid chain and the number following the colon, 0 in this case, is the number of double bonds on the fatty acid chain. Biodiesel fuels made from palm oil are ~40% C16:0, ~45% C18:1, and ~6% C18:2, and biodiesel fuels made from soybean oil are ~10% C16:0, ~25% C18:1, and ~55% C18:2. These FAMES are methyl laurate (C12:0, dodecanoic acid methyl ester; CAS number 111-82-0), methyl myristate (C14:0, tetradecanoic acid methyl ester; CAS number 124-10-7), methyl palmitate (C16:0, hexadecanoic acid methyl ester; CAS number 112-39-0), methyl oleate [C18:1, (z)-9-octadecanoic acid methyl ester; CAS number 112-62-9], methyl vaccinate [C18:1, (z)-11-octadecenoic acid methyl ester; CAS number 1937-63-9], and methyl linoleate [C18:2, (z,z)-9,12-octadecadienoic acid methyl ester; CAS number 112-63-0]. Table 1 shows that the melting point for methyl laurate, C12:0, is 4.3 (0.54) °C, the melting point for methyl palmitate, C18:0, is 28.48 (0.44) °C, and the melting point for methyl linolenate, C18:2, is −43.09 (0.71) °C.[19] Thus, the differences in cloud point temperatures exhibited by biodiesel fuels made from soybean, palm, and coconut oils are due to differences in the FAME composition and degree of saturation of the FAMEs. In Table 1, additional notation is included to indicate the position and orientation of the double bond(s), where $\Delta 9c$ is a double bond at the ninth carbon in the cis configuration.

A relatively new feedstock that is being investigated as a biodiesel fuel enhancer or extender is an oil derived from the seeds of cuphea (Lythraceae), a subtropical flowering plant native to the east central United States, Mexico, and Brazil.[2,20−27] There are approximately 260 species of cuphea.[2] Cuphea oil is similar to coconut oil in that it contains high concentrations of medium-chain fatty acids; however, cuphea oil contains over 65% (mass/mass) of capric acid, C10:0, which yields a nearly equivalent concentration of the FAME, methyl caprate (C10:0, decanoic acid methyl ester; CAS number 110-42-9) in the resulting biodiesel fuel.[19] While cuphea oil is not commercialized yet, cuphea has the advantage that it can be grown in temperate climates, including much of the United States. Thus, cuphea oil could directly compete with these imported sources (palm and coconut oils) for use as a biodiesel extender and as a domestic source of medium-chain fatty acids (e.g., lubricants, detergents, cosmetics, and confectionaries).[28] The impact of the shorter chain FAMEs of cuphea-derived biodiesel fuel on the resultant thermophysical properties must be determined and compared to those of other biodiesel fuels currently used (and proposed to be used) as an extender or enhancer (or possibly as a drop-in replacement) for petroleum-based diesel fuel. This

(16) Knothe, G. Dependence of biodiesel fuel properties on the structure of fatty acid alkyl esters. *Fuel Process. Technol.* **2005**, *86* (10), 1059–1070.

(17) Knothe, G.; Krahl, J.; Van Gerpen, J. *The Biodiesel Handbook*; Champaign, IL, 2004.

(18) Moser, B. R. Influence of blending canola, palm, soybean, and sunflower oil methyl esters on fuel properties of biodiesel. *Energy Fuels* **2008**, *22* (6), 4301–4306.

(19) Knothe, G.; Dunn, R. O. A comprehensive evaluation of the melting point of fatty acids and esters determined by differential scanning calorimetry. *J. Am. Oil Chem. Soc.* **2009**, *86* (9), 843–856.

(20) Knothe, G. ''Designer'' biodiesel: Optimizing fatty ester composition to improve fuel properties. *Energy Fuels* **2008**, *22* (2), 1358–1364.

(21) Geller, D. P.; Goodrum, J. W.; Knapp, S. J. Fuel properties of oil from genetically altered *Cuphea viscosissima*. *Ind. Crops Prod.* **1999**, *9* (2), 85–91.

(22) Cermak, S. C.; John, A. L.; Evangelista, R. L. Enrichment of decanoic acid in cuphea fatty acids by molecular distillation. *Ind. Crops Prod.* **2007**, *26* (1), 93–99.

(23) Graham, S. A.; Hirsinger, F.; Robbelen, G. Fatty acids of cuphea (Lythraceae) seed lipids and their systematic significance. *Am. J. Bot.* **1981**, *68* (7), 908–917.

(24) Gesch, R.; Forcella, F.; Olness, A.; Archer, D.; Hebard, A. Agricultural management of cuphea and potential for commercial production in the Northern Corn Belt. *Ind. Crops Prod.* **2006**, *24* (3), 300–306.

(25) Knapp, S. J.; Tagliani, L. A.; Roath, W. W. Fatty acid and oil diversity of *Cuphea viscosissima*—A source of medium-chain fatty acids. *J. Am. Oil Chem. Soc.* **1991**, *68* (7), 515–517.

(26) Vaughn, S. F.; Holser, R. A. Evaluation of biodiesels from several oilseed sources as environmental friendly contact herbicides. *Ind. Crops Prod.* **2007**, *26* (1), 63–68.

(27) Wolf, R. B.; Graham, S. A.; Kleiman, R. Fatty acid composition of cuphea seed oils. *J. Am. Oil Chem. Soc.* **1983**, *60* (1), 103–104.

(28) Forcella, F.; Gesch, R. W.; Isbell, T. A. Seed yield, oil, and fatty acids of cuphea in the Northwestern Corn Belt. *Crop Sci.* **2005**, *45* (6), 2195–2202.

comparison will aid in determining the applicability and suitability of cuphea-derived feedstocks designed for the production and manufacturing of biodiesel fuel.

Advanced Distillation Curve (ADC) Measurement. One of the most important and informative properties that is measured for complex fluid mixtures is the distillation (or boiling) curve.[29−31] Simply stated, the distillation curve is a graphical depiction of the boiling temperature of a fluid or fluid mixture plotted against the volume fraction distilled.[29−31] Distillation curves are typically associated with petrochemicals and petroleum refining.[32] Such curves are of great value in assessing the properties of any complex fluid mixture; indeed, the distillation curve is one of the few properties that can be used to characterize a complex fluid. Thus, distillation curves are used commonly in the design, operation, and specification of liquid fuels, such as gasoline, diesel fuel, rocket propellant, and gas turbine fuel.[33−35]

The most common presentation of the distillation curve is a plot of the boiling temperature (at ambient pressure) against the volume fraction. The standard test method, ASTM D-86, provides the usual approach to measurement, yielding the initial boiling point, the temperature at predetermined distillate volume fractions, and the final boiling point.[36] The ASTM D-86 test suffers from several drawbacks, including large uncertainties in temperature measurements and little theoretical significance.[37]

In earlier work, we described an improved method and apparatus for distillation curve measurement that is especially applicable to the characterization of fuels.[37−43] This method, called the ADC, is a significant improvement over current approaches, such as ASTM D-86. First, we

incorporate a composition-explicit data channel for each distillate fraction (for qualitative, quantitative, and trace analysis). Sampling very small distillate volumes ($5−25$ μL) yields a composition-explicit data channel with nearly instantaneous composition measurements. Chemical analysis of the distillate fractions allows for determination of how the composition of the fluid varies with the volume fraction and distillation temperature, even for complex fluids. These data can be used to approximate vapor−liquid equilibrium (volatility) of complex mixtures and presents a more complete picture of the fluid under study. The ADC approach provides consistency with a century of historical data, an assessment of the energy content of each distillate fraction, and where needed, a corrosivity assessment of each distillate fraction. Suitable analytical techniques include gas chromatography with either flame ionization detection (GC−FID), mass spectral detection (GC−MS), or element-specific detection (such as GC with sulfur or nitrogen chemiluminescence detection, GC−SCD or GC−NCD) and Fourier transform infrared spectrophotometry (FTIR).[44,45]

Another advantage of the ADC approach is that it provides temperature, volume, and pressure measurements of low uncertainty, and the temperatures obtained are true thermodynamic state points that can be modeled with an equation of state.[46−50] Such thermodynamic model development is simply impossible with the classical approach to distillation curve measurement. We have applied this metrology to hydrocarbon mixtures, azeotropic mixtures,

(29) Kister, H. Z. *Distillation Design*; McGraw-Hill: New York, 1991.

(30) Kister, H. Z. *Distillation Operation*; McGraw-Hill: New York, 1988.

(31) Leffler, W. L. *Petroleum Refining in Nontechnical Language*; PennWell: Tulsa, OK, 2000.

(32) Riazi, M. R. *Characterization and Properties of Petroleum Fractions, ASTM MNL50*; American Society for Testing and Materials (ASTM): West Conshohoken, PA, 2005.

(33) Manovyan, A. K.; Khachaturova, D. A.; Lozin, V. V. Method for determination of distillation curve of heavy petroleum products. *Chem. Technol. Fuels Oils* **1983**, *19* (5−6), 259−261.

(34) Karonis, D.; Lois, E.; Stournas, S.; Zannikos, F. Correlations of exhaust emissions from a diesel engine with diesel fuel properties. *Energy Fuels* **1998**, *12* (2), 230−238.

(35) Karonis, D.; Lois, E.; Zannikos, F.; Alexandridis, A.; Sarimveis, H. A neural network approach for the correlation of exhaust emissions from a diesel engine with diesel fuel properties. *Energy Fuels* **2003**, *17* (5), 1259−1265.

(36) American Society for Testing and Materials (ASTM). *ASTM Standard D 86-04b, Standard Test Method for Distillation of Petroleum Products at Atmospheric Pressure*; ASTM International: West Conshohocken, PA, 2004.

(37) Bruno, T. J. Improvements in the measurement of distillation curves—Part 1: A composition-explicit approach. *Ind. Eng. Chem. Res.* **2006**, *45*, 4371−4380.

(38) Bruno, T. J.; Smith, B. L. Improvements in the measurement of distillation curves—Part 2: Application to aerospace/aviation fuels RP-1 and S-8. *Ind. Eng. Chem. Res.* **2006**, *45*, 4381−4388.

(39) Smith, B. L.; Bruno, T. J. Improvements in the measurement of distillation curves: Part 3—Application to gasoline and gasoline + methanol mixtures. *Ind. Eng. Chem. Res.* **2007**, *46*, 297−309.

(40) Smith, B. L.; Bruno, T. J. Improvements in the measurement of distillation curves: Part 4—Application to the aviation turbine fuel Jet-A. *Ind. Eng. Chem. Res.* **2007**, *46*, 310−320.

(41) Smith, B. L.; Bruno, T. J. Advanced distillation curve measurement with a model predictive temperature controller. *Int. J. Thermophys.* **2006**, *27*, 1419−1434.

(42) Bruno, T. J. Method and apparatus for precision in-line sampling of distillate. *Sep. Sci. Technol.* **2006**, *41* (2), 309−314.

(43) Bruno, T. J.; Smith, B. L. Enthalpy of combustion of fuels as a function of distillate cut: Application of an advanced distillation curve method. *Energy Fuels* **2006**, *20*, 2109−2116.

(44) Bruno, T. J.; Ott, L. S.; Lovestead, T. M.; Huber, M. L. The composition explicit distillation curve technique: Relating chemical analysis and physical properties of complex fluids. *J. Chromatogr., A* **2010**, *1217*, 2703−2715.

(45) Bruno, T. J.; Ott, L. S.; Smith, B. L.; Lovestead, T. M. Complex fluid analysis with the advanced distillation curve approach. *Anal. Chem.* **2010**, *82* (3), 777−783.

(46) Huber, M. L.; Smith, B. L.; Ott, L. S.; Bruno, T. J. Surrogate mixture model for the thermophysical properties of synthetic aviation fuel S-8: Explicit application of the advanced distillation curve. *Energy Fuels* **2008**, *22*, 1104−1114.

(47) Huber, M. L.; Lemmon, E. W.; Diky, V.; Smith, B. L.; Bruno, T. J. Chemically authentic surrogate mixture model for the thermophysical properties of a coal-derived liquid fuel. *Energy Fuels* **2008**, *22*, 3249−3257.

(48) Huber, M. L.; Lemmon, E.; Kazakov, A.; Ott, L. S.; Bruno, T. J. Model for the thermodynamic properties of a biodiesel fuel. *Energy Fuels* **2009**, *23*, 3790−3797.

(49) Huber, M. L.; Lemmon, E.; Bruno, T. J. Effect of RP-1 compositional variability on thermophysical properties. *Energy Fuels* **2009**, *23*, 5550−5555.

(50) Huber, M. L.; Lemmon, E.; Ott, L. S.; Bruno, T. J. Preliminary surrogate mixture models for rocket propellants RP-1 and RP-2. *Energy Fuels* **2009**, *23*, 3083−3088.

(51) Bruno, T. J.; Wolk, A.; Naydich, A. Stabilization of biodiesel fuel at elevated temperature with hydrogen donors: Evaluation with the advanced distillation curve method. *Energy Fuels* **2009**, *23*, 1015−1023.

(52) Hadler, A. B.; Ott, L. S.; Bruno, T. J. Study of azeotropic mixtures with the advanced distillation curve approach. *Fluid Phase Equilib.* **2009**, *281*, 49−59.

(53) Bruno, T. J.; Wolk, A.; Naydich, A.; Huber, M. L. Composition explicit distillation curves for mixtures of diesel fuel with dimethyl carbonate and diethyl carbonate. *Energy Fuels* **2009**, *23* (8), 3989−3997.

(54) Bruno, T. J.; Wolk, A.; Naydich, A. Analysis of fuel ethanol plant liquor with the composition explicit distillation curve approach. *Energy Fuels* **2009**, *23* (6), 3277−3284.

(55) Bruno, T. J.; Wolk, A.; Naydich, A. Composition-explicit distillation curves for mixtures of gasoline with four-carbon alcohols (butanols). *Energy Fuels* **2009**, *23*, 2295−2306.

(56) Lovestead, T. M.; Bruno, T. J. Comparison of the hypersonic vehicle fuel JP-7 to the rocket propellants RP-1 and RP-2 with the advanced distillation curve method. *Energy Fuels* **2009**, *23* (7), 3637−3644.

(57) Lovestead, T. M.; Bruno, T. J. Application of the advanced distillation curve method to aviation fuel avgas 100LL. *Energy Fuels* **2009**, *23*, 2176−2183.

gasolines, diesel fuels (including biodiesel fuels), crude oils, aviation fuels, and rocket propellants.[37−40,42−45,51−72] Clearly, it is not always needed or desired to apply all aspects of the ADC metrology in every application. For example, for highly refined fuels, such as the low sulfur diesel fuels used today, it is usually unnecessary to assess corrosivity as a function of the distillate fraction.

In this paper, we apply the ADC method to compare biodiesel fuel samples produced from two very different seed oil feedstocks: one derived from soybeans (SME for soy methyl ester) and the other derived from the seed of the cuphea flower (CME for cuphea methyl ester). Specifically, we present the thermodynamically consistent distillation curve and use the composition-explicit data channel to characterize the curve in terms of composition and available energy content. We then compare the results to previous measurements performed for a neat biodiesel fuel obtained locally (B100) and an olive-oil-derived biodiesel fuel (IHP for in-house prepared).[63] For simplicity, we compare the biodiesel fuels presented here with just one representative B100 fuel from previous work and also with a petroleum-derived diesel fuel. Thus, we provide a basis of comparison among these fuels in terms of the fundamental thermophysical properties. These comparisons are critical in determining the applicability and suitability of cuphea oil feedstocks for use in producing biodiesel fuels for use as enhancers or extenders for petroleum diesel fuel.

Experimental Section

The *n*-hexane used as a solvent in this work was obtained from a commercial supplier and was analyzed with gas chromatography with flame ionization and/or mass spectrometric detection.[73−75] The *n*-hexane was injected with a syringe into a split/splitless injector set with a 100:1 split ratio. The injector was operated at a temperature of 325 °C and a constant head pressure of 69 kPa (10 psig). A 30 m capillary column of 5% phenyl−95% dimethyl polysiloxane, having a thickness of 1 μm, was used with a temperature-ramping program from 50 to 170 °C at a heating rate of 5 °C/min. These analyses revealed the purity to be approximately 99%, and the fluid was used without further purification.

The CME biodiesel fuel was obtained in collaboration with Sandia National Laboratories and originated from the National Center for Agricultural Utilization Research at the United States Department of Agriculture (USDA).[2] It was made from the refined bleached deodorized (RBD) oil from the cuphea germ-plasm line PSR 23 (*Cuphea viscosissima* × *Cuphea lanceolata*) obtained from cuphea seeds harvested from USDA plots in Morris, MN, and Peoria, IL.[2] The SME (CAS number 67784-80-9) biodiesel fuel was obtained from a commercial supplier. The SME fuel was used as a research fluid for previous engine testing.[76] These samples were stored tightly sealed in plastic bottles, and care was taken to minimize exposure to the atmosphere to limit oxidation, evaporation of the more volatile components, and the uptake of moisture. No other precautions were taken, nor were the samples physically or chemically dried. The SME sample was clear, and the CME sample was yellow.

The biodiesel fuel samples were subjected to chemical analysis before the measurement of the distillation curve. They were analyzed with GC−MS with a 30 m capillary column with a 0.1 mm coating of the stationary phase, 50% cyanopropyl−50% dimethyl polysiloxane. This stationary phase provides separations based on polarity and is specifically intended for the analysis of the FAME compounds that make up biodiesel fuels.[63] Samples were injected with a syringe into a split/splitless injector set with a 100:1 split ratio. The injector was operated at a temperature of 325 °C and a constant head pressure of 69 kPa (10 psig). A temperature program of 80 °C for 2 min followed by temperature ramping at 8 °C/min to 285 °C was used. The temperature was held at 285 °C for 5 min. Mass spectra were collected for each peak from 15 to 550 relative molecular mass (RMM) units. Peaks were identified with guidance from the NIST/EPA/NIH mass spectral database and also on the basis of retention indices.[73,75]

The method and apparatus for ADC measurements has been reviewed in detail elsewhere,[37−43] and thus, only a limited description is provided herein. In brief, 200 mL of each biodiesel fuel was placed into the boiling flask with a 200 mL volumetric pipet and an automatic pipetter for each distillation curve measurement. The thermocouples (T1 and T2) were inserted into the proper locations to monitor T_k, the temperature of the fluid in the kettle, and T_h, the temperature of the vapor at the bottom of the takeoff position in the distillation head (see Figure 1).

(58) Ott, L. S.; Smith, B. L.; Bruno, T. J. Advanced distillation curve measurements for corrosive fluids: Application to two crude oils. *Fuel* **2008,** *87,* 3055–3064.

(59) Ott, L. S.; Smith, B. L.; Bruno, T. J. Advanced distillation curve measurement: Application to a bio-derived crude oil prepared from swine manure. *Fuel* **2008,** *87,* 3379–3387.

(60) Ott, L. S.; Smith, B. L.; Bruno, T. J. Composition-explicit distillation curves of mixtures of diesel fuel with biomass-derived glycol ester oxygenates: A fuel design tool for decreased particulate emissions. *Energy Fuels* **2008,** *22,* 2518–2526.

(61) Ott, L. S.; Smith, B. L.; Bruno, T. J. Experimental test of the Sydney Young equation for the presentation of distillation curves. *J. Chem. Thermodyn.* **2008,** *40,* 1352–1357.

(62) Ott, L. S.; Hadler, A.; Bruno, T. J. Variability of the rocket propellants RP-1, RP-2, and TS-5: Application of a composition- and enthalpy-explicit distillation curve method. *Ind. Eng. Chem. Res.* **2008,** *47* (23), 9225–9233.

(63) Ott, L. S.; Bruno, T. J. Variability of biodiesel fuel and comparison to petroleum-derived diesel fuel: Application of a composition and enthalpy explicit distillation curve method. *Energy Fuels* **2008,** *22,* 2861–2868.

(64) Smith, B. L.; Ott, L. S.; Bruno, T. J. Composition-explicit distillation curves of diesel fuel with glycol ether and glycol ester oxygenates: A design tool for decreased particulate emissions. *Environ. Sci. Technol.* **2008,** *42* (20), 7682–7689.

(65) Smith, B. L.; Ott, L. S.; Bruno, T. J. Composition-explicit distillation curves of commercial biodiesel fuels: Comparison of petroleum derived fuel with B20 and B100. *Ind. Eng. Chem. Res.* **2008,** *47* (16), 5832–5840.

(66) Bruno, T. J.; Laesecke, A.; Outcalt, S. L.; Seelig, H.-D.; Smith, B. L. Properties of a 50/50 mixture of Jet-A + S-8. NIST-IR-6647, 2007.

(67) Ott, L. S.; Bruno, T. J. Corrosivity of fluids as a function of distillate cut: Application of an advanced distillation curve method. *Energy Fuels* **2007,** *21,* 2778–2784.
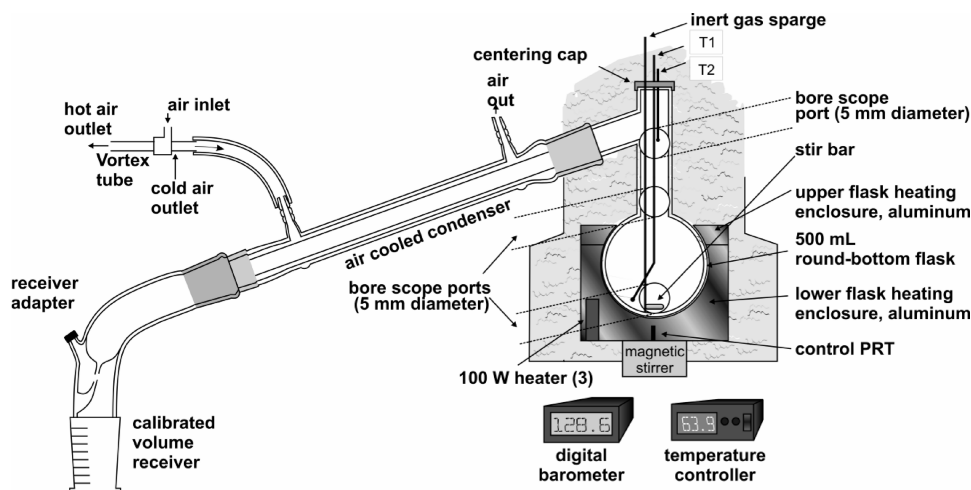
(68) Ott, L. S.; Bruno, T. J. Modifications to the copper strip corrosion test for the measurement of microscale samples. *J. Sulfur Chem.* **2007,** *28* (5), 493–504.

(69) Bruno, T. J. Thermodynamic, transport and chemical properties of "reference" JP-8. Book of Abstracts, Army Research Office and Air Force Office of Scientific Research, 2006 Contractor's Meeting in Chemical Propulsion, 2006; pp 15−18.

(70) Bruno, T. J.; Huber, M. L.; Laesecke, A; Lemmon, E. W.; Perkins, R. A. Thermochemical and thermophysical properties of JP-10, NIST-IR 6640. National Institute of Standards and Technology (NIST), Boulder, CO, 2006.

(71) Smith, B. L.; Bruno, T. J. Composition-explicit distillation curves of aviation fuel JP-8 and a coal-based jet fuel. *Energy Fuels* **2007,** *21,* 2853–2862.

(72) Smith, B. L.; Bruno, T. J. Application of a composition-explicit distillation curve metrology to mixtures of Jet-A + synthetic Fischer−Tropsch S-8. *J. Propul. Power* **2008,** *24* (3), 619–623.

(73) Bruno, T. J.; Svoronos, P. D. N. *CRC Handbook of Fundamental Spectroscopic Correlation Charts*; CRC Press, Inc.: Boca Raton, FL, 2005.

(74) Lide, D. R. *CRC Handbook of Chemistry and Physics*, 85th ed.; CRC Press, Inc.: Boca Raton, FL, 2004−2005.

(75) National Institute of Standards and Technology (NIST)/Environmental Protection Agency (EPA)/National Institutes of Health (NIH) Mass Spectral Database. SRD Program, NIST, Gaithersburg, MD, 2005.

(76) Mueller, C. J.; Boehman, A. L.; Martin, G. C. An experimental investigation of the origin of increased NO_x emissions when fueling a heavy-duty compression-ignition engine with soy biodiesel. *SAE Int. J. Fuels Lubr.* **2009,** *2* (1), 789–816.

Figure 1. Schematic diagram of the overall apparatus used for the measurement of distillation curves.

Enclosure heating was then commenced with a four-step program based on a previously measured distillation curve.[63] Volume measurements were made in a level-stabilized receiver, and sample aliquots were collected at the receiver adapter hammock. Because oxidative degradation of the FAME components of biodiesel fuel is known to occur,[51] we placed a sparge tube into the distillation kettle and bubbled argon into the fluid for 15 min with stirring (see Figure 1) before applying heat (commencing the distillation). In prior work, we demonstrated that this procedure yields highly reproducible distillation curve results.[63,77] After 15 min, the sparge tube was removed from the fluid to avoid affecting the fluid temperature during the distillation and positioned directly above the fluid. An argon purge of the atmosphere above the fluid was maintained throughout the distillation at a flow rate of 5 mL/min.

Because the measurements of the distillation curves were performed at ambient atmospheric pressure (typically ∼83 kPa), temperature readings were corrected for what should be obtained at standard atmospheric pressure (1 atm = 101.325 kPa). The average experimental atmospheric pressure for the ADC measurements presented herein was 83.1 kPa. The uncertainty in the pressure measurement is 0.003 kPa. The pressure corrections were performed with the modified Sydney Young equation, in which the constant term was assigned a value of 0.000 109.[78−80] This value corresponds to a *n*-alkane carbon chain of 12.[63] Some comments regarding this assignment are in order. In our implementation of the modified Sydney Young equation, we use a constant that is specific for the chain length being measured. The constants were determined by a regression of available experimental data, which, unfortunately, do not extend to very large hydrocarbon chains.[37] Clearly, biodiesel fuel is better represented by a hydrocarbon chain length greater than 12. We chose not to use a predicted value for the constant term (for a larger chain) in our data presentation to be consistent with previous measurements and with measurements on petroleum-derived diesel fuel. We note, however, that, for a carbon chain of 18, the predicted constant would be 0.000 095; use of this value (in place of that for a chain length of 12) would lower the presented temperatures

uniformly by 1.2 °C. The shapes of the distillation curves would be unchanged. The magnitude of the Sydney Young correction depends upon the extent of the deviation from standard atmospheric pressure.[61] The location of the laboratory in which the measurements were performed is approximately 1650 m above sea level, resulting in a typical temperature adjustment of ∼7 °C.

To provide the composition channel information to accompany the temperature data grid on the distillation curves, sample aliquots were withdrawn for 12 selected distillate volume fractions. To accomplish this, aliquots of ∼7 µL of emergent fluid were withdrawn from the sampling hammock in the receiver adapter with a blunt-tipped chromatographic syringe and added to a crimp-sealed vial containing a known mass (∼1 mL) of *n*-hexane solvent. A sample was withdrawn at the first drop of fluid from the condenser and then at each of 11 additional volume fractions of distillate, for a total of 12 sample aliquots. Each distillate volume aliquot underwent two analyses. First, each aliquot was subjected to chemical analysis and peak identification by GC−MS, as described above for the analyses of the neat biodiesel fuel samples.[73−75] Once the compounds in each aliquot were identified, the aliquots were analyzed with GC−FID with external standards to determine the compounds. Aliquots (3 µL) from crimp-sealed vials of each sample were injected with an automatic sampler. High-purity nitrogen was used as the carrier and makeup gas. The split/splitless injection inlet was maintained at 300.0 °C. The column and temperature program were identical to those of the GC−MS analysis. The FID was maintained at 275.0 °C. After standardization, an enthalpy of combustion

(77) Bruno, T. J.; Wolk, A.; Naydich, A. Stabilization of biodiesel fuel at elevated temperature with hydrogen donors: Evaluation with the advanced distillation curve method. *Energy Fuels* **2009**, *23* (1), 1015–1023.
(78) Young, S. Correction of boiling points of liquids from observed to normal pressures. *Proc. Chem. Soc.* **1902**, *81*, 777.
(79) Young, S. *Fractional Distillation*; Macmillan and Co., Ltd.: London, U.K., 1903.
(80) Young, S. *Distillation Principles and Processes*; Macmillan and Co., Ltd.: London, U.K., 1922.

(81) Rowley, R. L.; Wilding, W. V.; Oscarson, J. L.; Zundel, N. A.; Marshall, T. L.; Daubert, T. E.; Danner, R. P. DIPPR Data Compilation of Pure Compound Properties. Design Institute for Physical Properties AIChE, New York, NY, 2004.
(82) Brown, R. L.; Stein, S. E. Boiling point data. In *NIST Chemistry WebBook, NIST Standard Reference Database Number 69*; Linstrom, P. J., Mallard, W. G., Eds.; NIST: Gaithersburg, MD (http://webbook.nist.gov).
(83) *CRC Handbook of Data on Organic Compounds*, 2nd ed.; Weast, R. C., Grassellik, J. G., Eds.; CRC Press, Inc.: Boca Raton, FL, 1989; p 1.
(84) *Catalog Handbook of Fine Chemicals*; Aldrich Chemical Company, Inc.: Milwaukee, WI, 1990.
(85) Erickson, D.; Wilding, W. V.; Oscarson, J. L.; Rowley, R. L. Use of the DIPPR database for development of QSPR correlations: Normal boiling point. *J. Chem. Eng. Data* **2002**, *47*, 1293–1302.
(86) Krop, H. B.; van Velzen, M. J. M.; Parsons, J. R.; Govers, H. A. J. Determination of environmentally relevant physical-chemical properties of some fatty acid esters. *J. Am. Oil Chem. Soc.* **1997**, *74* (3), 309–315.
(87) Rakoff, H.; Emken, E. A. Synthesis and properties of methyl 9,12,15-octadecatrienoate geometric isomers. *Chem. Phys. Lipids* **1982**, *31* (3), 215–225.

Table 2. Listing by Retention Time (RT) of the Components of SME Identified by GC–MS and Determined by GC–FID[a]

RT (min)	compound	CAS number	RMM	area (%)
15.1	methyl palmitate	112-39-0	270.45	10.9
17.0	methyl stearate	112-61-8	298.50	4.2
17.3	methyl oleate	112-62-9	296.49	24.3
17.8	methyl linoleate	112-63-0	294.47	54.1
18.3	methyl linolenate	301-00-8	292.46	6.5

[a] RMM is the relative molecular mass of the compound.

Table 3. Listing by RT of the Components of CME Identified by GC–MS and Determined by GC–FID[a]

RT (min)	compound	CAS number	RMM	area (%)
5.0	methyl caprylate	111-11-5	158.24	0.5
7.6	methyl caprate	110-42-9	186.29	74.3
11.1	methyl laurate	111-82-0	214.34	3.3
13.4	methyl myristate	124-10-7	242.40	3.5
15.1	methyl palmitate	112-39-0	270.45	5.0
17.0	methyl stearate	112-61-8	298.50	0.5
17.3	methyl oleate	112-62-9	296.49	8.0
17.8	methyl linoleate	112-63-0	294.47	5.0

[a] RMM is the relative molecular mass of the compound.

analysis that has been described in detail previously[43] was performed on the biodiesel fuel distillate fractions corresponding to 0.025, 10, 50, and 80% of the distillate volume.

Results and Discussion

Chemical Composition. The chemical compositions of SME and CME were identified with GC–MS and subsequently determined by GC–FID. The main components of the SME biodiesel fuel (see Table 2) were five FAMEs: methyl palmitate, methyl stearate, methyl oleate, methyl linoleate, and methyl linolenate. These five FAMEs account for 100% (mass/mass) of the SME composition. The SME composition was compared to two previously measured samples, a B100 sample that was obtained from a commercial source and the IHP sample that was prepared in-house.[63] These three biodiesel fuels, B100, IHP, and SME, are made up of primarily the same five FAMEs in the same relative proportions.[63] In a recent paper that used ^{1}H nuclear magnetic resonance (NMR) (500 MHz) to characterize the FAME composition of SME, methyl vaccenate (an isomer of methyl oleate) was found to make up 1.5% of the FAME composition (see Table 1).[9]

The main components of the CME biodiesel fuel (see Table 3) were six FAMEs: methyl caprate, methyl laurate, methyl myristate, methyl palmitate, methyl oleate, and methyl linoleate. Very small concentrations of methyl stearate and methyl caprylate (C8:0, octanoic acid methyl ester; CAS number 111-11-5) were also identified, but each made up less than 0.6% (mass/mass) of the total composition. More than 80% of the CME biodiesel fuel thus consists of FAMEs that are shorter in carbon chain length than any of the FAMEs identified in the SME, B100, and IHP biodiesel fuels. It is important to note that the FAME analysis presented in Table 3 reports a higher concentration of methyl caprate than the fatty acid profile of cuphea oil reported previously by Knothe and co-workers.[2] When we compare the uncalibrated area percents (not reported in Table 3), however, they are in very good agreement with their data. The influence of the compositional differences exhibited by the SME and CME fuels on the distillation curves and enthalpies of combustion will be discussed below.

Table 4. Comparison of the Initial Boiling Temperatures of SME and CME[a]

sample (pressure) (kPa)	sustained bubbling (°C)	vapor rise (°C)
SME (82.5 kPa)	328.2	**349.6**
CME (83.5 kPa)	234.6	**245.9**

[a] These temperatures have been corrected to 1 atm (101.325 kPa) with the Sydney Young equation. The pressures at which the measurements were made are provided in the first column to permit recovery of the actual measured temperature. The uncertainties are discussed in the text.

Initial Boiling Behavior. In the course of this work, we performed between four and six measurements of complete distillation curves for each biodiesel fuel. During the initial heating of the SME and CME biodiesel fuels in the distillation flask, the behavior of the fluid was carefully observed. Direct observation through the flask window or through the bore scope (see Figure 1) allowed for measurement of the onset of boiling for each of the mixtures (measured with T_k). For the ADC method, we typically record the temperatures at which we visually observe (a) the first bubble, (b) sustained bubbling, and (c) the temperature at which vapor is observed to rise into the distillation head. This latter temperature, the vapor rise temperature, is observed with a sharp increase in the temperature of T_h. We have shown that the vapor rise temperature is the theoretically significant initial boiling temperature (IBT) of the mixture. This temperature is highlighted in bold in Table 4 and can be used in the development of an equation of state. During the initial heating of the biodiesel fuels, prior to the observation of the first bubble, the fuels transition in color from clear or yellow to a darker color. The darker color of these fluids is expected; however, it makes observation of the initial bubbling temperature difficult. Thus, we report only the temperatures at which we observed sustained bubbling and the vapor rise temperature. The uncertainty (with a coverage factor $k = 2$) of the initial boiling temperature measurements has been discussed in detail in previous papers and is typically approximately 2.0 °C for the first bubble and sustained bubbling temperatures and approximately 0.2 °C for the vapor rise temperature.[62] The uncertainty of those temperatures for biodiesel fuel is somewhat higher. With the sparge tube procedure, however, the uncertainty in the biodiesel fuel temperature measurements in the fluid is decreased to 5.0 °C in the sustained bubbling temperature and 0.5 °C in the vapor rise temperature.

Sustained bubbling was observed for a representative SME distillation when the temperature of the fluid reached 328.2 °C and the vapor rise temperature was 349.6 °C. For a representative CME distillation, sustained bubbling was observed when the temperature of the fluid reached 234.6 °C and the vapor rise temperature was 245.9 °C. These temperatures have been corrected to standard atmospheric pressure with the modified Sydney Young equation as described above; the experimental pressures are provided, so that the actual temperatures measured can be recovered.

The temperature values obtained for the soybean-derived biodiesel fuel, SME, are remarkably similar to those obtained previously for both the B100 and the olive-oil-derived, IHP biodiesel fuel.[63] The vapor rise temperatures reported for these two biodiesel fuels ranged from 350.2 to 352.9 °C. Interestingly, the sustained bubbling and the vapor rise temperatures measured for the cuphea-derived biodiesel fuel, CME, were ~100 °C lower than those for SME, B100, and IHP. The significantly lower boiling temperatures for CME are due to the relatively higher concentration of light

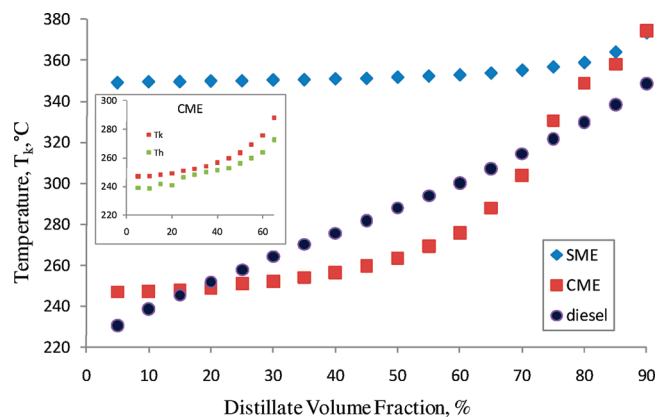**Table 5. Representative Distillation Curve Data of SME and CME**[a]

distillate volume fraction (%)	SME (°C) (82.5 kPa)		CME (°C) (83.5 kPa)	
	T_k	T_h	T_k	T_h
5	350.5	348.4	247.1	239.1
10	351.0	348.8	247.2	238.7
15	351.1	349.1	248.2	241.8
20	351.4	349.3	249.1	241.0
25	351.5	349.4	251.0	246.5
30	351.9	349.4	252.4	248.2
35	352.0	349.4	254.1	249.9
40	352.4	349.3	256.6	251.5
45	352.6	349.9	259.6	252.9
50	353.2	350.0	263.5	256.2
55	353.7	350.7	269.3	260.0
60	354.3	350.4	275.8	263.9
65	355.1	351.5	288.1	272.8
70	356.5	352.4	303.8	279.8
75	358.2	354.7	330.6	291.2
80	360.2	355.8	348.9	334.7
85	365.3	357.8	358.0	343.2
90	374.5	358.9	374.6	345.9

[a] These data are plotted in Figure 2. The uncertainties are discussed in the text. These temperatures have been corrected to 1 atm (101.325 kPa) with the Sydney Young equation. The experimental pressures for these measurements are provided.


Figure 2. Representative distillation curves of SME and CME presented as T_k (the temperature measured in the fluid). The distillation curve for a representative diesel fuel sample that was measured previously is also presented.[63] The inset presents T_k and T_h (the temperature measured in the head) to illustrate possible azeotropic convergence. Although only one curve for each fluid is shown, each curve was measured 4 times. The uncertainties are discussed in the text and are smaller than the symbols used.

components in CME compared to that of SME. Tables 2 and 3 show that ~80% (mass/mass) of CME was composed of FAMEs that were shorter than those found in the SME fluid. While the vapor rise temperature for CME differs significantly from the vapor rise temperatures observed for the other biodiesel fuels (SME, B100, and IHP), it is remarkably similar to the vapor rise temperature for petroleum-derived diesel fuel, which was reported at 233.4 °C.[63] The lower boiling temperature for CME indicates that it may retain some of the superior engine performance properties of petroleum-derived diesel fuel versus SME, such as more rapid vaporization in-cylinder. The differences in the initial boiling temperatures of CME and SME are further illustrated with distillation curves.

Distillation Curves. Representative distillation curve data for SME and CME are provided in Table 5 for both the fluid temperature (T_k) and the temperature in the distillation head (T_h). The T_k data are true thermodynamic state points, while the T_h data allow for a comparison to historical measurements. These temperatures have been corrected to standard atmospheric pressure with the Sydney Young equation as described above; the experimental pressures were provided to recover the actual temperatures measured. The estimated uncertainty (with a coverage factor $k = 2$) in the temperatures reported in this table is 0.5 °C. Table 5 shows that T_h lags T_k by a few degrees Celsius for each distillate volume fraction.

Figure 2 shows graphically the distillation data for SME and CME in terms of T_k (the temperature in the fluid) for the same distillations presented in Table 5. The distillation curve for a representative petroleum-derived diesel fuel sample that was measured previously is also presented.[63] The uncertainty bars on the fluid temperature measurements are smaller than the symbols used. The temperature range from 5 to 90% distillate volume fraction for CME spans 130 °C, whereas for SME, this temperature range spans only 25 °C. Interestingly, the 90% distillate volume fractions for both CME and SME were collected at the same temperature (374.5 °C) as shown in Table 5 and Figure 2. At low distillate volume

fractions, early in the distillation curves, the boiling temperature differences are observed because CME is significantly richer in lighter FAMEs. Specifically, Tables 2 and 3 show that over 70% (mass/mass) of CME is composed of methyl caprate (RMM = 186.29), whereas almost 50% (mass/mass) of SME is composed of methyl linoleate (RMM = 294.47), and larger molecular-mass molecules within the same chemical family tend to distill at higher temperatures. Methyl stearate (RMM = 298.50) is the largest FAME observed, and it was identified in both CME at 0.5% (mass/mass) and SME at 4.2% (mass/mass), hence the overlap in the distillation curves at the last distillate volume fraction. The diesel fuel spans a similar temperature range to that of CME; however, the cuphea-derived biodiesel fuel distillation reached higher temperatures than those for the petroleum-derived diesel fuel. For example, the 85% distillate fraction for the petroleum-derived diesel fuel boiled at ~330 °C, whereas the same fraction for the CME sample boiled at 358.0 °C.[63] Also, the diesel fuel distilled at a temperature ~15 °C lower than that for CME at the 5% distillate volume fractions.

The shape of the distillation curve can also provide valuable information about the fuel mixture. For example, the distillation curve of a pure fluid is flat, and the distillation curve for SME is relatively flat throughout the distillation. This behavior is because more than 80% (mass/mass) of the SME composition is from FAMEs with 19 carbons (methyl stearate, methyl oleate, methyl linoleate, and methyl linolenate) and ~12% (mass/mass) is from methyl palmitate, a FAME with 17 carbons. These FAMEs are almost identical in structure and RMM, and thus they have very similar boiling points (see Table 1) and exhibit a narrow distillation temperature range (see Table 5 and Figure 2). Additionally, T_k and T_h differ throughout this distillation by only 3 °C until the 55% distillate volume fraction, another characteristic typical of fluids that are made up of compounds from the same moiety family that are similar in RMM.

Figure 2 shows that the CME distillation curve has an initial gradual rise in temperature until ~50% distillate volume fraction. At higher distillate volume fractions, the slope rises much more rapidly. The relationship between T_k and T_h can be seen in the inset of Figure 2 for the CME

(a) SME Biodiesel Fuel

(b) CME Biodiesel Fuel
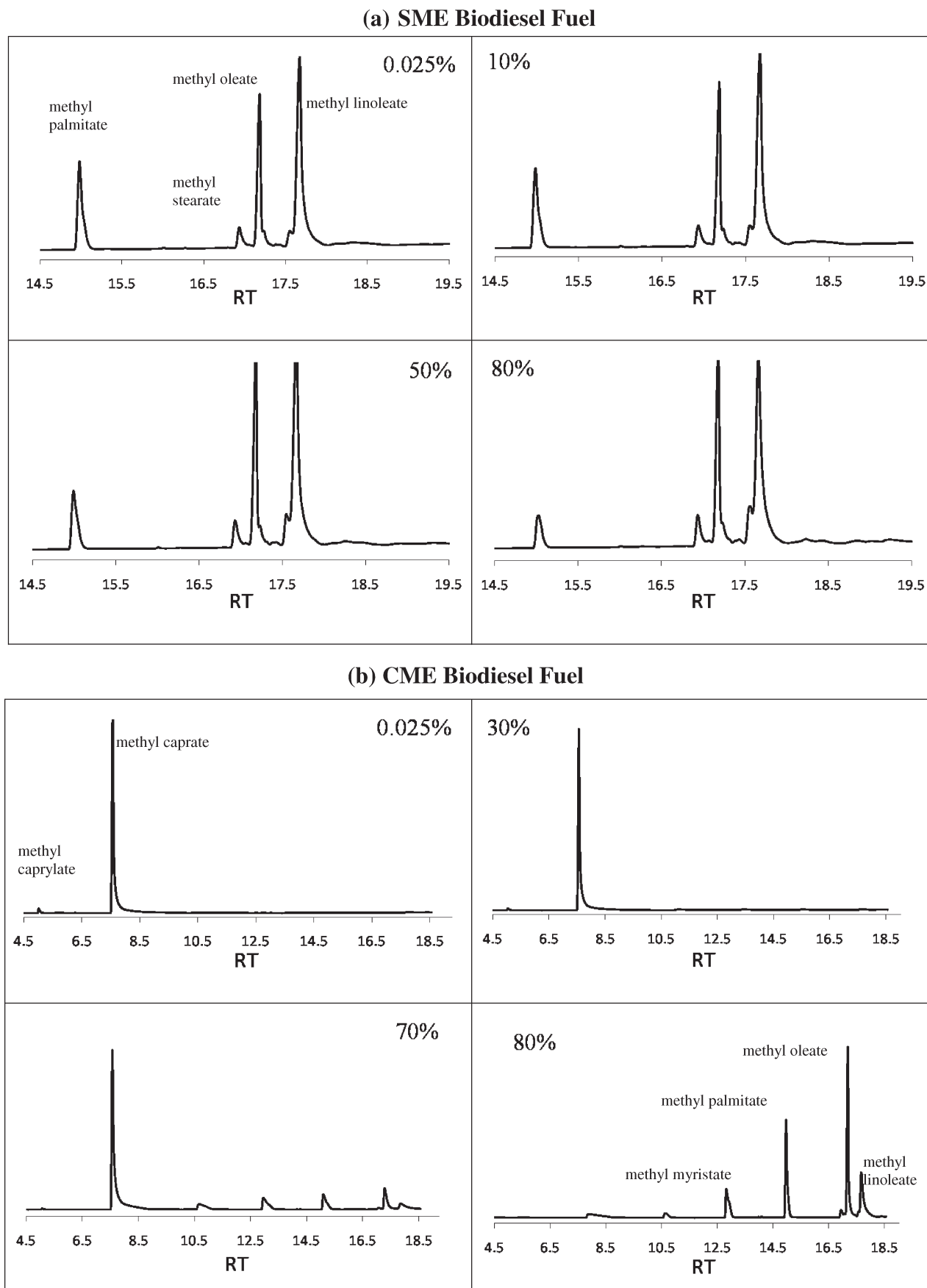
Figure 3. (a and b) Representative chromatograms of four distillate volume fractions of SME and CME. The major FAME peaks are labeled in the first fraction in which they were observed. The *y* axes are arbitrary units of intensity, and the *x* axes are RT in minutes. The details of the chromatography are discussed in the text.

distillation that is presented in Table 5. The inset shows that, in the initial part of the distillation curve, the slope of the curve is gradual and T_k and T_h converge from ∼20 to 50% distillate volume fractions. This convergence can indicate either the distillation of a pure component (unlikely to be the cause, because several FAMEs remain in the kettle) or the formation of an azeotrope, a phenomenon that has been observed in numerous mixtures.[39,52] We stress that we have no other indications of azeotropy for this mixture, with the literature being currently silent on such mixtures. It thus remains a topic of further investigation. There was no indication of azeotropy for either the SME biodiesel fuel or the petroleum-derived diesel fuel.

Composition Channel Information. While the gross examination of the distillation curves is instructive and valuable for many design purposes, the composition channel of the ADC approach can provide more information that can aid in developing a better understanding of the thermophysical behavior of the fluid. One can sample and examine the individual fractions as they emerge from the condenser. Representative chromatograms for each fraction of the emergent fluid of both SME and CME are shown in panels a and b of Figure 3. The RT axis is in minutes for each chromatogram, and the abundance axis is presented in arbitrary units of area counts (voltage slices). The solvent (*n*-hexane) appears at the front of each chromatogram. Its peak does not interfere with the sample and was removed digitally.

Both panels a and b of Figure 3 show that the lightest components decrease in concentration (peak area) throughout the distillation. For example, Figure 3a shows that the peak for methyl palmitate in SME decreases more relative to the larger FAMEs in each distillate volume fraction presented. Additionally, methyl caprate was the only component identified in the first drop of CME, and this FAME was nearly absent from the 80% distillate volume fraction (see Figure 3b). Analogous to the lightest components decreasing in concentration throughout the distillation, it is also often observed that the heavier/larger components increase in concentration (peak area) throughout the distillation. For example, the larger FAMEs (methyl palmitate, methyl oleate, and methyl linoleate) were first observed in low quantities in the 70% distillate volume fraction from the CME distillation. These FAMEs were observed in each of the SME distillate volume fractions with increasing concentrations throughout the distillation. The presence of these larger FAMEs in the first drop from the SME distillation in much higher amounts to those in CME helps to explain the much higher boiling temperatures observed for SME.

The composition channel of the ADC also provides insight into the shape of the CME distillation curve. Figure 3b shows that 0.025 (the first drop), 30, and 70% distillate volume fractions are made up of almost exclusively methyl caprate. In the 50% distillate volume fraction (not shown in Figure 3b), the larger FAMEs appear in minor concentrations. The appearance of these larger FAMEs corresponds to the end of the T_h and T_k convergence and the dramatic increase in the slope of the distillation curve. As the distillation progresses beyond the convergence, the larger FAMEs begin to increase in concentration. Figure 3b shows a very dramatic change in the CME distillate volume composition from 70 to 80%. Specifically, in the 70% distillate volume fraction, methyl caprate is still the predominant component and the larger FAMEs are present in minor concentrations.

Table 6. Total Enthalpy of Combustion, Presented in −kJ/mol, of Four Distillate Volume Fractions of SME and CME, along with B100 and the Olive-Oil-Derived Biodiesel Fuel, IHP, that were Investigated Previously for Comparison[63] [a]

distillate volume fraction (%)	SME	CME	B100	IHP
0.025	10788 (356)	6397 (211)	10403 (343)	10610 (350)
10	10807 (357)	6405 (211)	10468 (345)	10650 (351)
50	10867 (359)	6534 (216)	10579 (349)	10742 (355)
80	10928 (361)	9708 (320)	10689 (353)	10910 (360)

[a] The uncertainties are presented in parentheses.
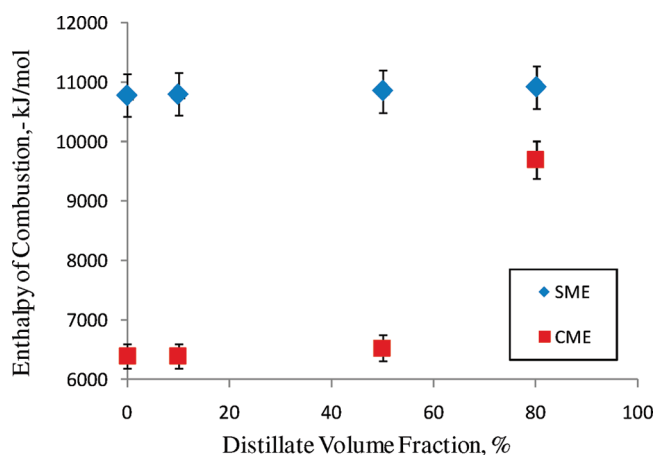
Figure 4. Enthalpy of combustion for the biodiesel fuels SME and CME presented at four distillate cuts: 0.025 (the first drop), 10, 50, and 80%. The uncertainties are discussed in the text.

In the 80% distillate volume fraction, the methyl caprate concentration drops to ∼6% of the fluid and the mixture is composed mostly of the larger FAMEs (methyl oleate, methyl palmitate, and methyl linoleate). The similarity in the composition of CME and SME of the 80% distillate volume fractions explains how the distillation curves of SME and CME overlap at high distillate volume fractions. Last, Figure 3b shows a very small peak that is present in low concentration in each distillate volume fraction, except for the 80% distillate volume fraction. This small peak is methyl caprylate. It is possible that the extremely small concentration of methyl caprylate [less than 0.5% (mass/mass)] contributes to the interesting distillation behavior exhibited by the CME fluid.

Enthalpy of Combustion. The composition-explicit data channel allows for the addition of thermochemical data to the distillation curve.[39,40,43,55] We have discussed the contributions to the overall uncertainty of the total enthalpy of combustion elsewhere.[39,40,43,63] The main sources of uncertainty in the enthalpy of combustion calculation here are due to (1) uncertainty in the values tabulated for the individual enthalpy of combustion values for each component, (2) uncertainty in the measured mole fraction, and (3) uncertainty arising from the absence of data for experimental enthalpy of combustion for some of the constituents. There is also uncertainty in neglecting the enthalpy of mixing of FAMEs; however, this value has been shown previously to contribute to less than 0.01% of the enthalpy of combustion of FAME mixtures.[63] Additionally, there may be uncertainty in the enthalpy of combustion because of the inability to resolve very closely related isomers via the analytical protocol, the complete misidentification of a component,

Table 7. Total Enthalpy of Combustion, Presented in −kJ/g and −kJ/L, of Four Distillate Volume Fractions of SME and CME, along with B100 That Was Investigated Previously for Comparison[63] [a]

distillate volume fraction (%)	mass basis			volume basis		
	SME (−kJ/g)	CME (−kJ/g)	B100 (−kJ/g)	SME (−kJ/L)	CME (−kJ/L)	B100 (−kJ/L)
0.025	37 (1)	34 (1)	36 (1)	32737 (1080)	29776 (983)	31517 (1040)
10	37 (1)	34 (1)	36 (1)	32754 (1081)	29782 (983)	31502 (1040)
50	37 (1)	34 (1)	36 (1)	32811 (1083)	29867 (986)	31663 (1045)
80	37 (1)	37 (1)	37 (1)	32869 (1085)	31913 (1053)	31772 (1049)

[a] The uncertainties are presented in parentheses.

and neglecting components present at very low concentrations; however, both SME and CME contain a small number of easily resolved and identified peaks, and thus, these contributions are also negligible. In past work, we determined that neglecting peaks with total uncalibrated area percentages of up to 4% increased the uncertainty of the calculated enthalpy by only 1.5%.[43] Thus, neglecting minor components in the biodiesel fuel distillate fractions does not significantly affect the uncertainty of the total enthalpy of combustion. In view of these sources of uncertainty, the overall combined uncertainty in our total enthalpy of combustion calculations (with a coverage factor $k = 2$) was 3.3%.[63] The uncertainty is dominated by the analytical measurement and determination of the component mole fractions.

The total enthalpy of combustion (which we represent as $-\Delta H_c$) can be found by multiplying the enthalpy of combustion of each of the pure (or individual) components by the mole fraction of that component and then adding the contributions of the individual components to obtain the total enthalpy of combustion[39,40,43]

$$-\Delta H_c = \sum x_i(-\Delta H_i) \qquad (1)$$

where i refers to the individual components that have been identified or selected and the enthalpy of mixing is ignored.[39,40,43]

The total enthalpy of combustion of both SME and CME (taking into account peaks with area percentage in excess of 2%) was calculated at four distillate volume fractions: 0.025 (the first drop), 10, 50, and 80%. Table 6 and Figure 4 present the calculated enthalpies of combustion, in −kJ/mol, for the distillate volume fractions of SME and CME. For comparison, the previously determined enthalpies of combustion for B100 and the olive-oil-derived biodiesel fuel, IHP, are also presented in Table 6.[63] For simplicity, we compare the biodiesel fuels presented herein to just one representative B100 fuel from previous work. At each distillate volume fraction measured, the total enthalpies of combustion on a per mole basis for the B100, IHP, and SME samples are very close, within the uncertainty of the measurement, and are significantly higher than for the CME sample.[63] These results are consistent with the distillation curve measurements (Figure 2). Lower vaporization temperatures generally correspond to lower concentrations of larger molecules. Table 6 shows that the molar enthalpy of combustion dramatically increases for CME in the 80% distillate volume fraction. This result is consistent with the results shown in Figure 3b, which show that the larger FAMEs are in only the 70 and 80% distillate volume fractions. Table 1 shows that the larger saturated FAMEs boil at higher temperatures. Thus, on a per mole basis, the 70 and 80% CME distillate volume fractions provide more energy than the earlier distillate volume fractions.

The presentation of the thermochemical information in units of −kJ/mol is useful for design and modeling studies, because thermochemical information presented in this way represents fundamental values easily applied to the individual component mole fractions. A practical engineering alternative would be to present $-\Delta H_c$ in terms of mass or volume, expressed in −kJ/g or −kJ/L, respectively. The conversion to a per mass basis requires only the RMM of the constituents of each sample; the uncertainty of this calculation remains at 3.3%. Table 7 shows that the distillate fractions presented for B100 and SME have an equivalent per mass basis enthalpy. The 80% distillate fractions for each biodiesel fuel have an equivalent per mass basis enthalpy; however, the earlier distillate fractions for CME are lower on a per mass basis enthalpy than those for SME.

Presentation of the data on a per volume basis is also valuable. Consumers are more accustomed to thinking about fuel on a per volume basis instead of a per mole or per mass basis. The conversion to a per volume basis requires both the RMM and the density of the constituents of each sample at each distillate temperature. Here, reliable density data of the constituents of each sample are available as a function of the distillation temperatures, and the uncertainty of this calculation remains at 3.3%.[81] Table 7 shows that, as with the per molar basis comparisons, the distillate fractions presented for B100 and SME have an equivalent per volume basis enthalpy. The 80% distillate fractions for each biodiesel fuel also have an equivalent per volume basis enthalpy, and once again, the earlier distillate fractions for CME are lower on a per volume basis enthalpy than for SME.

Conclusions

The soybean-derived biodiesel fuel, SME, and the cuphea-derived biodiesel fuel, CME, were measured with the ADC metrology. The results were compared to the previously investigated commercially available biodiesel fuel, B100, and the olive-oil-derived, in-house prepared biodiesel fuel, IHP. Comparisons to petroleum-derived diesel fuel were also made. The distillation curve of the CME biodiesel fuel is very different from those exhibited by SME, B100, and IHP. The CME biodiesel fuel is significantly more volatile at lower fractions, akin to the behavior previously observed for petroleum-derived diesel fuel. The SME and CME biodiesel fuels exhibited the same volatility and composition after 80% distillate volume fraction. We also observed evidence of azeotropy during the CME distillation at lower distillate volume fractions. The temperatures measured are true thermodynamic state points that can be used to model each fluid with an equation of state. The ADC metrology allowed for a

detailed, fraction-by-fraction chemical analysis of both the SME and the CME biodiesel fuel, including calculation of the total enthalpies of combustion of each distillate fraction. The distillate fractions presented for B100 and SME have an equivalent enthalpy of combustion on a molar, mass, and volume basis. The 80% distillate fractions for each biodiesel fuel have an equivalent per mass basis enthalpy; however, the earlier distillate fractions for CME are lower on a molar, mass, and volume basis enthalpy than for SME.